Temperature Compensated AlN Based SAW

Andrew B. Randles, Julius M. Tsai, Piotr Kropelnicki, and Hong Cai
Institute of Microelectronics, A*STAR (Agency for Science, Technology and Research),
11 Science Park Road, Singapore Science Park II, Singapore 117685
Email: randlesab@ime.a-star.edu.sg

***Abstract*—Surface acoustic wave (SAW) devices are used in many areas of telecommunications, and other areas where precise filtering is need. New devices and specification require tighter control of the filtering devices. This is a problem for SAW filters because they often have a large temperature coefficient. Some crystal cuts of quartz can manage the temperature affects and there have been other methods proposed to compensate for the temperature affects of some SAW devices. In this paper a novel method of SAW temperature compensation is proposed consisting of oxide trenches in a silicon substrate for an AlN SAW device. Along with the oxide trenches changes in the oxide trench sidewall angle allow for the adjustment of the second order TCF of the device. Using simulations the first order TCF was reduced from -26.7 ppm to 0 and it was possible to reduce the second order TCF from -24.7 ppb to -1.8 ppb.**

***Index Terms*—aluminum nitride, temperature compensation, AlN SAW, surface acoustic wave**

I. Introduction

Surface acoustic wave (SAW) devices have been in use for some time as filters in TVs, cell phones, radar arrays and many other applications. They are attractive for their relative ease of manufacture and their filtering characteristics which are almost completely controlled by device design. The main drawback of these devices is the temperature instability of filters and resonators. This is a function of the temperature coefficients of elasticity (TCE), coefficients of thermal expansion (CTE) and the CTE's affect on density.

Currently, temperature compensation is achieved by several methods. One is to use a crystal cut of quartz that is inherently temperature stable. The drawback of this method is that there are second order temperature coefficients that are not automatically compensated for [1]. Another method is to use external temperature compensation circuits to meet the specification needed for the filter. This has the disadvantage that it cannot be employed with passive SAW sensors. Also, new IEEE requirements for temperature stability require 10 ppm temperature stability over the entire temperature range [2].

There are several methods being used currently to compensate acoustic wave (AW) devices. Most devices make use of silicon dioxide's (SiO2), oxide, positive TCE to compensate other materials' negative TCE and CTE. One set of authors used oxide as a cladding material with SAW devices to compensate TCE and CTE of the piezoelectric substrate [3]. Another paper used oxide to compensate aluminum nitride (AlN) based Lamb wave device. In this device oxide is applied to the underside of a suspended AlN membrane. They were able to achieve a close to zero temperature coefficient of frequency (TCF) for the first order temperature effects [4], [5]. In another paper, oxide pillars were added to a bulk acoustic wave (BAW) resonator to remove the first order temperature affects for the TCF. This was only localized because there were still second order temperature effects in the device which gave the device an overall performance of 83 ppm for 120 ℃ temperature range, [6], [7]. While that is much better than other BAW device it does not meet the requirements of the IEEE standard [2].

Two other temperature compensation methods developed involved adding a heater underneath a zinc oxide (ZnO) SAW device [8]. With the addition of the heater, the temperature of the SAW material could be controlled and maintained. This device has the disadvantage that it is not a passive method of temperature compensation; consequently it cannot be used in passive sensors and the device is not CMOS compatible. A second paper changes the properties of the AlN film by doping it [9]. The doped AlN layer has positive TCE coefficients making zero TCF structures possible. The downside of this method is it does not allow for custom devices on the same die with different TCF and there may be affects on the quality of resonator produced.

The device proposed here is a unique structure that will make it possible to achieve a 0 TCF for first order effects and control the second order effects by device geometry. This is accomplished by adding trenches filled with oxide under the SAW wave and controlling the shape of those trenches.

II. Device Structure

A typical AlN SAW device is shown in Fig. 1 along with the FEA solution found in COMSOL. That analysis shows that the device has a first order TCF of -26.7 ppm and a second order TCF of -24.7 ppb. Therefore, the equation determining the frequency as a function of temperature would be as shown in equation (1).

$$F(T) = F_0(1 - 26.7 * 10^{-6} * \Delta T - 24.7 * 10^{-9} * \Delta T^2) \quad (1)$$

Manuscript received February 28, 2013; revised May 28, 2013

doi: 10.12720/joace.2.2.191-194

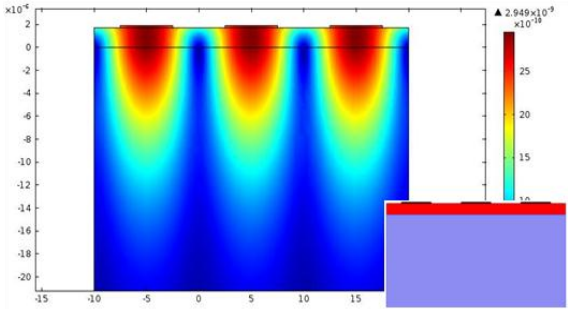

Figure 1. Standard AlN SAW device operating at 250 MHz. Its 1st order TCF is -26.7 ppm and its 2nd order coefficient is -24.7 ppb.

Accordingly, for a 1 ℃ change in temperature and a 250 MHz device, the change in frequency would be -6.7 kHz, 26.8 ppm, and over 100 ℃ change the frequency shift would be -729 kHz, 2,916 ppm. These simulations are based on material properties found in the following papers [6], [10].

For the research described here, shown in Fig. 2 and Fig. 3 the oxide trench is placed between the electrodes in a periodic fashion to match the operating frequency of the device.

III. Device Simulations

One strategy for doing the simulations is to look at the TCF, to analyze the TCE and temperature effects on density, and then to use these details to determine the correct trench dimension. Equation (2) is the calculation of the TCF for a homogenous material only considering first order components [4].

$$TCF = \frac{1}{2}[TCE - (\alpha_{11} + \alpha_{22} + \alpha_{33})] - \alpha_z \qquad (2)$$

This equation is only for first order TCF effects and it is for a homogenous material. In order to apply it to the structure proposed here, approximations would need to be made that account for the different materials and geometries in the device. In a separate example of a BAW wave device oxide pillars were used in the vibrating medium to compensate for the temperature effects [6], [7]. They found the best volume ratio, equation (3), to compensate for the first order TCF affects [5].

$$1 \leq \frac{V_{SiO_2} * TCE_{SiO_2}}{V_{Si} * TCE_{Si}} \left(\frac{E_{SiO_2}}{E_{Si}} + \sqrt{\frac{\rho_{SiO_2}}{\rho_{Si}} \Big/ \frac{E_{SiO_2}}{E_{Si}}} \right) \leq 3 \qquad (3)$$

This equation cannot be applied to the trench structure proposed here for several reasons. First, most of the energy of the SAW is contained in the first wavelength of the wave and does not penetrate much further into the substrate. Finally, it will be shown later, but the geometry of the trenches is shown to have an impact on the TCF. An expression to determine the optimum trench dimensions may be proposed in future work; in this work temperature compensation is considered for two different frequencies.

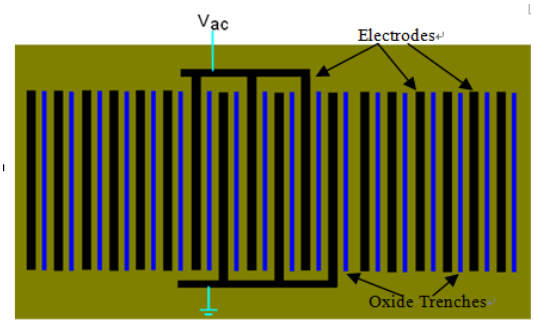

Figure 2. Electrode and oxide trench configuration for a standard SAW and variable electrode device. The black represents electrodes and the blue represents oxide trenches under the AlN.

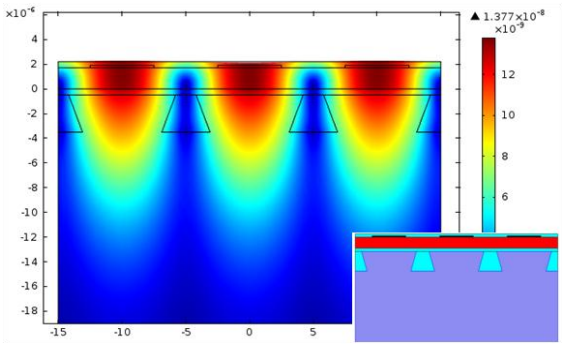

Figure 3. AlN SAW device with oxide trenches. The trapezoid has a top and bottom ration of 0.3. Its 1st order TCF is 0.8 ppm and its 2nd order coefficient is -1.8 ppb. Further variation of the trapezoid ratio is shown in Fig. 7.

Simulations were carried out using COMSOL with the basic device structure shown in Fig. 1 and Fig. 3 with component thicknesses shown in Table I and materials constants listed in Table II. The data that was reported in [10] was used to extract the temperature coefficients for AlN used in the simulations. No temperature dependent data for Al was included because this is heavily dependent on the methods used to deposit the Al and the impurities in the Al.

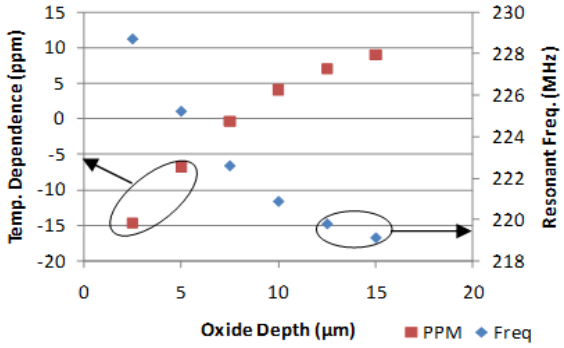

Figure 4. Variation in oxide trench depth with respect to the TCF and the resonant frequency of the device.

Initially, the investigation focused on the effects of the trench depth and trench width on the TCF and resonant frequency of the SAW. In Fig. 4 and Fig. 5 it can be seen that the TCF increases due to the increase in trench depth/width and the resonant frequency decreases. The

additional oxide with its positive TCE will increase the TCF. The lower acoustic velocity of oxide will also lowers the resonant frequency of the device.

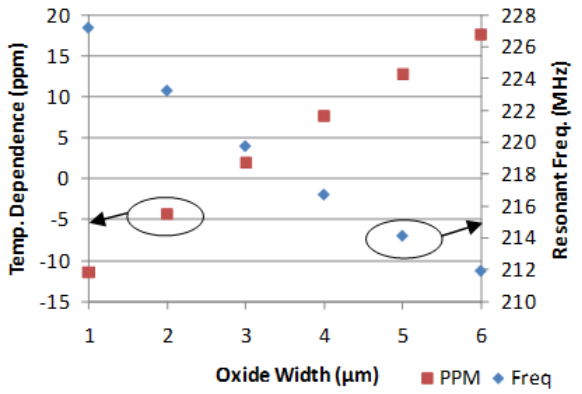

Figure 5. Variation in oxide trench width for a constant trench depth of 3.5 µm.

TABLE I. PARAMETERS USED IN SIMULATION

Parameter	Value
AlN thickness	1.7 µm
Top and Bottom Oxide thickness	50 nm
Electrode Thickness	20 nm
Electrode width and gap	5 µm or 10 µm
Left and Right Boundary Conditions	Anti-Perodic
Bottom boundary condition	Fully fixed

TABLE II. MATERIAL CONSTANTS USED FROM [6] AND [10]

		AlN	Si	SiO_2	Al
elastic constants, c_{ij} [GPa]	c_{11}	410.06	170	70	70
	c_{12}	100.69			
	c_{13}	83.82			
	c_{33}	386.24			
	c_{44}	100.58			
	c_{66}	154.70			
1st order TCE Tc_{ij} [10^{-6}/K]	Tc_{11}	-10.65	-63	204	-
	Tc_{12}	-11.67			
	Tc_{13}	-11.22			
	Tc_{33}	-11.13			
	Tc_{44}	-10.82			
	Tc_{66}	-10.80			
2nd order TCE $T2c_{ij}$ [10^{-9}/K^2]	$T2c_{11}$	-20.61	-52	221	-
	$T2c_{12}$	-19.51			
	$T2c_{13}$	-19.88			
	$T2c_{33}$	-20.03			
	$T2c_{44}$	-20.36			
	$T2c_{66}$	-20.39			
piezoelectric stress coef., e_{ij} [C/m]	e_{15}	-0.48	-	-	-
	e_{31}	-0.58			
	e_{33}	1.55			
relative permittivity, ε_{ij}	ε_{11}	9	11.7	4.2	-
	ε_{33}	11	11.7	4.2	
CTE, α_{ij} [10^{-6}/K]	α_{11}	5.27	2.6	0.55	18
	α_{33}	4.15	2.6	0.55	18
density, ρ [kg/m^3]		3260	2329	2200	2700

Next, a series of simulations were run with different trench dimensions that have 0 TCF for the first order TCF for two different electrode widths, Fig. 6. This shows that for different operating frequencies there are different optimum oxide trenches in order to achieve a zero TCF. This is likely due to the penetration depth of the acoustic wave into the substrate. The shorter wavelengths are more influenced by the top and bottom oxides cladding the AlN.

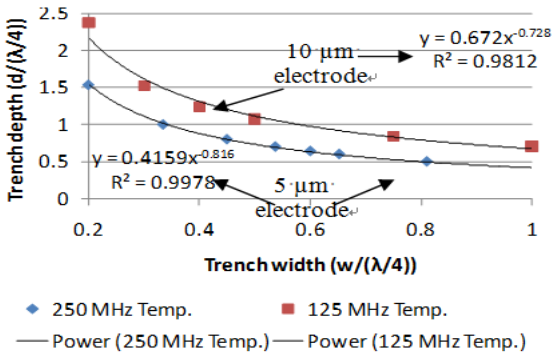

Figure 6. Trench dimensions for rectangular trenches to achieve 1st order 0 ppm TCF. Axes are normalized with respect to λ/4 which is equal to the electrode width.

Finally, the oxide sidewall angle in the simulations was changed. This was done while maintaining the same cross sectional area of the oxide trenches, Fig. 7. From that analysis it was seen the second order TCF was changed along with the first order TCF by changing the ratio of the trapezoidal oxide trench. This shows that the second order TCF can be controlled by an additional design parameter. The need for the negative slope of the oxide trench is most likely due to how the oxide sidewall follows the shape of the area with minimum energy.

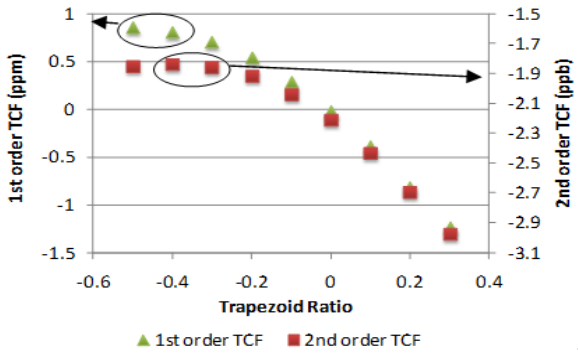

Figure 7. 1st and 2nd order variation due to change in the trapezoid ratio. Trapezoid dimensions are 3 µm deep and on average 2.7 µm wide and a device with a 5 µm electrode pitch.

IV. DISCUSSION

One result from the simulations is that the amount of oxide needed to compensate the structure is dependent on the wavelength of the wave and how much AlN and oxide there is on the surface. This is to be expected based because most of the SAW energy trapped is in the surface energy penetrate deeper into the Si substrate and is less affected by the top oxide on the device. In future work the relationship between operating frequency, AlN

thickness and the amount of oxide needed to fully temperature compensate the structure can be investigated by both COMSOL simulation and by analytical methods, using equations (2) and (3) as a starting point.

One note to consider with all of the simulations performed is that they are based on numbers found in literature. A device fabricated at a different foundry or lab could have significantly different material properties, thus changing what the optimum structure is for achieving 0 TCF. Analyses will need to be done on structures fabricated to determine the material constants there, especially the second order TCE and thermal expansion coefficients.

V. Conclusion

In this work, a new method for designing temperature compensated SAW devices with AlN and oxide trenches is described. This basic design could be extended to other piezoelectric devices materials on Si such as ZnO or PZT. By adding different shapes to the trench oxide used for temperature compensation it is possible to tune the first and second order TCF coefficients. Using this technique it is possible to achieve close to 0 TCF for both first and second order TCF coefficients. This is an improvement over most other passive methods to give temperature compensation because it addresses the second order TCF.

This work was supported by the Science and Engineering Research Council of A*STAR (Agency for Science, Technology and Research), Singapore, under grant number: 1021650084.

References

[1] D. Hauden, M. Michel, and J. J. Gagnepain, "Higher order temperature coefficients of quartz SAW oscillators," in *Proc. Frequency Control Symposium, 1978 IEEE International*, 1978, pp. 77-86.

[2] *IEEE Std 802.16-2004, IEEE 802.16™: Broadband Wireless Metropolitan Area Networks (MANs).* 2004

[3] C. B. Willingham, T. E. Parker, and F. H. Spooner, "Temperature compensated surface acoustic wave devices," US Patent 3,965,444, June 22, 1976.

[4] J. H. Kuypers, C.-M. Lin, G, Vigevani, and A, P. Pisano, "Intrinsic temperature compensation of aluminum nitride lamb wave resonators for multiple-frequency references," in *Proc. Frequency Control Symposium 2008 IEEE International*, 2008, pp. 240-2498.

[5] T. T. Yen, C. M Lin, X. Zhao, V. V. Felmetsger, D. G. Senesky, M. A. Hopcroft, and A. P. Pisano, "Characterization of aluminum nitride lamb wave resonators operating at 600 ℃ for harsh environment RF applications," in *Proc. Micro Electro Mechanical Systems, 2010 IEEE 23rd International Conference on*, 2010, pp. 731-734.

[6] R. Tabrizian, M. Pardo, and F. Ayazi, "A 27 MHz temperature compensated MEMS oscillator with sub-ppm instability," in *Proc. MEMS Conference 2012*, 2012, pp. 23-26.

[7] F. Ayazi, R. Tabrizian, and G. Casinovi, "Methods of forming micromechanical resonators having high density trench arrays therein that provide passive temperature compensation," US Patent Application, 2010.

[8] O. Tigli and M. E. Zaghloul, "Temperature stability analysis of CMOS-SAW devices by embedded heater design," *IEEE Transactions on Device and Materials Reliability*, vol. 8 no. 4, pp. 705-713, Dec. 2008.

[9] K. Tsubouchi and N. Mikoshiba, "Zero-temperature-coefficient SAW devices on A1N epitaxial films," *IEEE Transaction on Sonics and Ultrasonics*, vol. 32 no. 5, pp. 634-644, Sept. 1985.

[10] D. K. Pandey and R. R. Yadav, "Temperature dependent ultrasonic properties of aluminium nitride," *Applied Acoustics*, vol. 70, no. 3, pp. 412-415, Mar. 2009.

Andrew B. Randles was born in upstate New York in the USA in Jan 1979. He received his bachelors and masters degrees in mechanical engineering from Rochester Institute of Technology, Rochester, NY, USA in 2002. He received his PhD in nanomechanics from Tohoku University, Sendai, Japan in 2007. He is currently working as a research scientist at the Institute of Microelectronics in Singapore, A*STAR (Agency for Science, Technology and Research). Dr. Randles is a member of IEEE and ASME.

Julius Ming-Lin Tsai was born in Taipei, Taiwan, R.O.C., in June 1976. He received the B.S. and Ph.D. degrees in power mechanical engineering from National Tsing Hua University, Hsin-Chu, Taiwan, in 1995 and 2004, respectively. From June 2003 to April 2004, he was a visiting scholar with Carnegie–Mellon University, Pittsburgh, PA, where he was involved with mechanical-noise dominated CMOS accelerometers. From 2004 to 2009 he joined VIA Technologies, where he was involved with high-frequency small-signal modeling. He was a principle investigator in Institute of Microelectronics, Singapore and an adjunct assistant professor with Department of Electrical and Computer Engineering, National University of Singapore. His main research focus in IME was in RFMEMS, NEMS switch, MEMS ultrasound transducers (cMUT) and ruggedized MEMS sensors utilizing the advantage of silicon and AlN. Dr. Tsai was the recipient of a scholarship presented by the National Science Council of Taiwan. He is now working with Invensense Inc.

Piotr Kropelnicki was born in Leszno (Poland) on 20.Sep.1981. Piotr Kropelnicki received his Diplom Ingenieur degree in electrical and electronics engineering in 2007 from Universität Duisburg-Essen, Germany with major on microelectronics. Piotr Kropelnicki finished his Ph.D. degree in microelectronics at Fraunhofer Institute for Microelectronic Circuit and Systems, in 2010. He is currently a principal investigator, leading a team in SAM – Sensors & Actuators Microsystems Program at the Institute of Microelectronics. He is responsible for the development of several sensors operating in harsh environment, like pressure, gas detection, optical, viscosity and temperature sensors.

Hong Cai received the B.Eng. and M.Eng. degrees from Xi'an Jiaotong University, Xi'an, China, in 1997 and 2000, respectively and the Ph.D. degree from Nanyang Technological University, Singapore in 2009. She is currently a Research Scientist with the Institute of Microelectronics, A*STAR (Agency for Science, Technology and Research), Singapore. Her research interests include optical and photonics MEMS/NEMS, nano-sensors development.

